JACS
JOURNAL OF THE AMERICAN CHEMICAL SOCIETY
Article
pubs.acs.org/JACS

Feasibility of Intramolecular Proton Transfers in Terpene Biosynthesis – Guiding Principles

Young J. Hong and Dean J. Tantillo*

Department of Chemistry, University of California Davis, One Shields Avenue, Davis, California 95616, United States

Supporting Information

ABSTRACT: On the basis of results from quantum chemical calculations, the feasibility of an extensive series of intramolecular proton-transfer reactions postulated to occur during terpene biosynthesis is assessed and guiding principles are proposed.

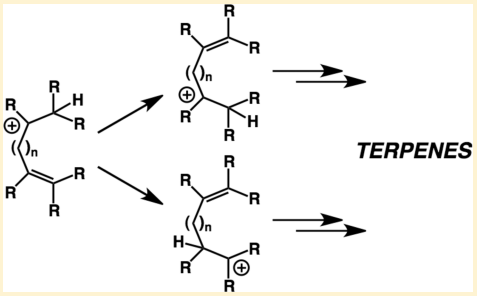

INTRODUCTION

The movement of hydrogen atoms from their locations in oligoprenyl diphosphate precursors to terpenes (e.g., geranyl, farnesyl, geranylgeranyl diphosphate) to new locations in terpene natural products is a common occurrence in terpene biosynthesis.[1] Most of these hydrogen migrations have been formulated as intramolecular hydride transfers to carbenium ion centers or as deprotonation/reprotonation processes, but, from time to time, intramolecular proton transfers have also been proposed. In recent years, several theoretical and experimental reports have provided new evidence for the feasibility of such proton-transfer mechanisms (*vide infra*). Herein, the lines of evidence put forth in these reports are assessed critically in light of previously reported experiments, and the limitations of the methodologies employed and the results of new computations on additional systems are described. This analysis has led to guiding principles for predicting the feasibility of intramolecular carbon-to-carbon proton transfers.

Proposed intramolecular proton transfers involved in terpene-forming carbocation cycloisomerizations/rearrangements are shown in Figure 1 (some of these are proposed in the literature, as referenced below, but others are proposed by us herein). We have organized these into four groups: (a) those involved in sesquiterpene-forming processes initiated by ionization of farnesyl diphosphate (FPP); (b) those involved in diterpene-forming processes initiated by ionization of geranylgeranyl diphosphate (GGPP); (c) those involved in diterpene-forming processes initiated by ionization of copalyl diphosphate (CPP); and (d) those involved in the biomimetic synthesis of the triterpene alcohol, germanicol. The predicted barriers for the proton-transfer reactions shown will each be discussed in turn, followed by a discussion of the general principles governing their magnitudes. Note that all of these reactions can be thought of as transfers of protons between two C=C π-bonds, but they differ in the length of the alkyl tethers between the π-bonds and whether the π-bonds are endo- or exocyclic with respect to the cycle (or bicycle) formed transiently as the proton migrates. While these proton-transfer reactions can all, in principle, be accomplished via deprotonation/reprotonation pathways, we focus herein on the feasibility of direct transfer without enzymatic intervention; in effect, we predict which systems would require such intervention and which would not.

METHODS

Calculations were performed with Gaussian 03 and Gaussian 09.[2] Geometries were optimized using the B3LYP/6-31+G(d,p) method,[3] and all stationary points were characterized by frequency calculations. Reported energies include zero-point energy corrections (unscaled) from B3LYP/6-31+G(d,p) calculations. Intrinsic reaction coordinate (IRC) calculations also were used to characterize transition-state structures.[4] mPW1PW91/6-31+G(d,p)//B3LYP/6-31+G(d,p)[5] and MPWB1K/6-31+G(d,p)//B3LYP/6-31+G(d,p)[6] energies are included for comparison, since B3LYP has been shown to underestimate the relative energies of cyclic structures versus acyclic isomers.[5,7] These methods have been used extensively to study terpene-forming carbocation rearrangements.[7] Atom numbers in all structures are based on standard atom numbering for terpene precursors. Structural drawings were produced using Ball & Stick;[8] ball-and-stick drawings of some transition structures reported in previous papers are not reproduced herein. The shortest contacts between migrating H's and the C=C units between which they migrate are shown as red dashed lines in Figures 2–8. Other selected distances are shown as black dashed lines.

RESULTS AND DISCUSSION

Trichodiene. In 2006, density functional theory (DFT) computations on part of the carbocation rearrangement leading to the sesquiterpene natural product trichodiene (Figure 1a)

Received: December 13, 2014
Published: March 12, 2015

DOI: 10.1021/ja512685x
J. Am. Chem. Soc. 2015, 137, 4134–4140

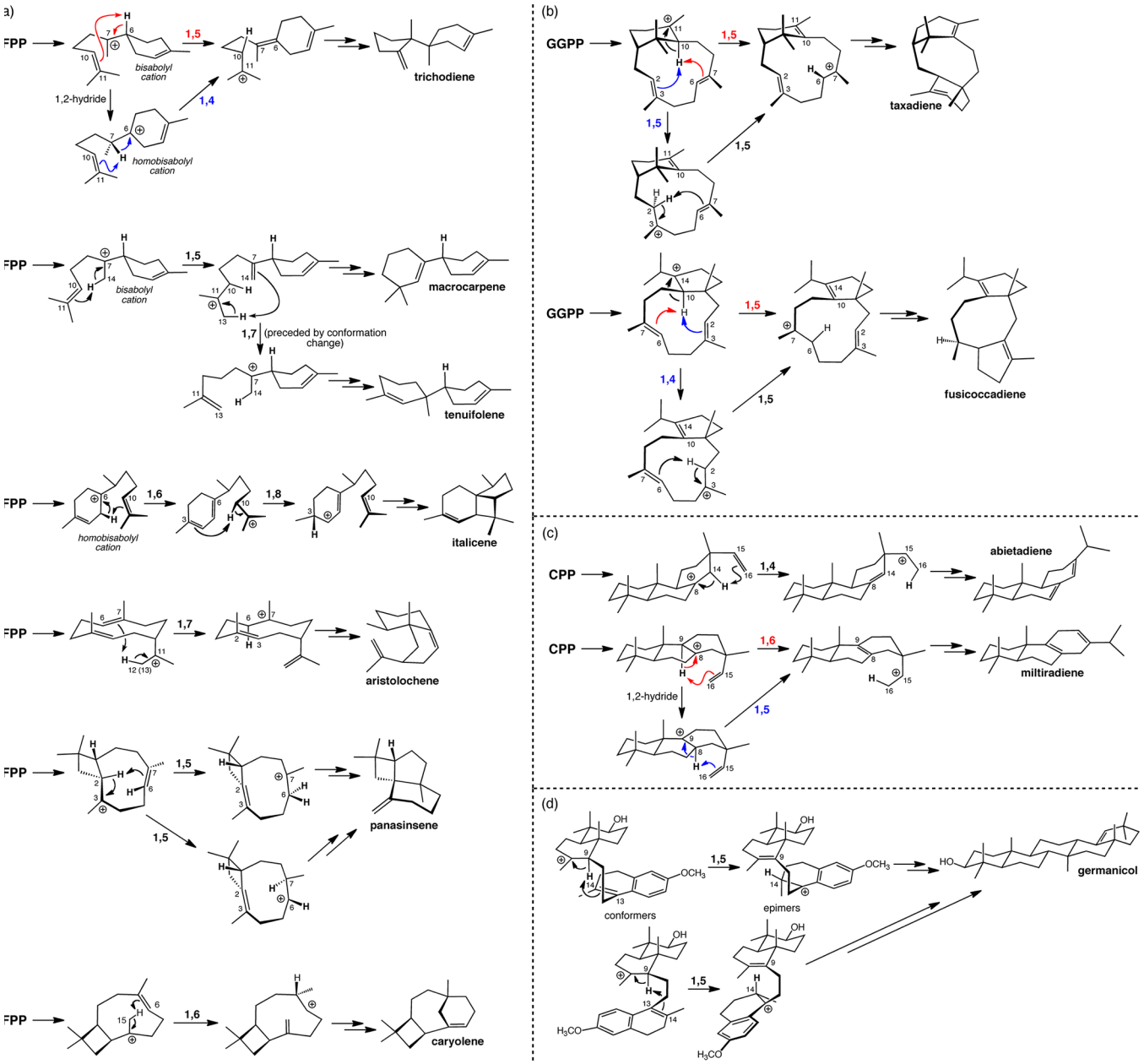

Figure 1. Proposed intramolecular proton transfers involved in carbocation rearrangements leading to terpenes. (a) Sesquiterpene-forming rearrangements initiated by the ionization of FPP. (b) Diterpene-forming rearrangements initiated by the ionization of GGPP. (c) Diterpene-forming rearrangements initiated by the ionization of CPP. (d) Intramolecular proton transfers involved in a biomimetic synthesis of germanicol.

were described.[9] Although mechanisms involving hydride transfer rather than proton transfer were previously proposed,[10] the quantum chemical calculations indicated such pathways were associated with much higher activation barriers (at least in the absence of the enzyme active site) than was a pathway involving a 1,5-proton transfer (~20 kcal/mol from the bisabolyl cation vs <10 kcal/mol; Table 1). In a subsequent study,[11] a 1,4-proton-transfer alternative (preceded by a 1,2-hydride shift) was found to have a very similar barrier. The prediction that proton-transfer pathways are inherently preferred over hydride-transfer pathways for this system is true at the levels of theory examined previously and reported for the first time herein (Table 1). The proton-transfer pathways proposed based on the results of the quantum chemical calculations are consistent with all reported experiments on trichodiene synthase.[9−11]

Macrocarpene and Tenuifolene. Macrocarpene and tenuifolene[12] can also be derived from the bisabolyl cation via intramolecular proton-transfer reactions (Figure 1a). While trichodiene can arise from initial transfer of the proton at the tertiary carbon (C6) connected to the carbocation center, macrocarpene can arise from initial transfer of a proton from the attached methyl group (C14; Figure 2, left). The latter proton transfer is associated with a slightly higher barrier than is the former (Table 1). The resulting carbocation (after a conformational change) could then, in principle, undergo a 1,7-proton transfer en route to tenuifolene, but this proton-transfer process is predicted to be coupled asynchronously into a concerted process with a preceding ring fragmentation event and a subsequent cyclization event (Scheme 1) that is associated with a much higher barrier (Table 1; this reaction is also predicted to be endothermic by 5−7 kcal/mol). This

DOI: 10.1021/ja512685x
J. Am. Chem. Soc. 2015, 137, 4134−4140

Table 1. Computed Barriers (kcal/mol) for Intramolecular Hydrogen-Transfer Reactions[a]

terpene	mechanism	method			proton transfer proposed in
		B3LYP	mPW1PW91	MPWB1K	
trichodiene	1,5-proton	8.05	4.96	6.14	ref 9
	1,2-hydride	6.08	3.51	1.47	
	1,4-proton	7.62	5.17	7.28	ref 11
	1,4-hydride	**30.44**	**27.82**	**26.74**	
macrocarpene	1,5-proton	12.26	9.86	11.57	this work
tenuifolene	**1,7-proton**	**27.28**	**30.90**	**34.85**	this work
italicene	1,6-proton	6.78	6.05	10.97	this work
	1,8-proton	19.21	17.20	16.88	
aristolochene	**1,7-proton (*si/si*)**	**25.42**	**21.79**	**22.32**	ref 15
	1,7-proton (*re/si*)	**25.65**	**23.12**	**25.18**	
panasinsene	1,5-proton (to C6)	15.31	12.63	11.55	this work
	1,5-proton (to C7)	3.88	1.92	4.37	
caryolene	**1,6-proton**	**21.50**	**24.90**	**24.46**	ref 22
taxadiene	1,5-proton (C10 to C6)	13.17	11.00	12.42	ref 24
	1,5-proton (C10 to C2)	8.50	6.50	8.44	ref 23
	1,5-proton (C2 to C6)	7.37	5.52	6.92	
fusicoccadiene	1,5-proton (C10 to C6)	16.00	13.48	15.55	this work
	1,4-proton (C10 to C2)	8.87	6.91	9.72	ref 25
	1,5-proton (C2 to C6)	3.99	1.50	4.29	
abietadiene	**1,4-proton (*re/re*, conformer 1)[b]**	**28.05**	**26.29**	**29.47**	ref 27
	1,4-proton (*re/si*, conformer 1)[b]	**29.58**	**28.07**	**31.08**	
	1,4-proton (*re/re*, conformer 2)[b]	**30.40**	**28.41**	**31.35**	
	1,4-proton (*re/si*, conformer 2)[b]	**31.11**	**29.32**	**32.46**	
miltiradiene	1,2-hydride (*re/si*)	1.27	−0.11	−1.25	ref 28
	1,6-proton (*re/re*)	13.65	10.95	12.81	
	1,2-hydride (*re/si*)	2.24	−0.10	−1.38	
	1,5-proton (*re/si*)	14.15	11.30	12.86	
germanicol	1,5-proton (*re/si*)	7.92	7.50	7.04	ref 30
	1,5-proton (*re/re*)	8.59	6.48	8.22	
	1,4-proton	18.07	16.03	18.29	

[a]Predicted barriers ≥20 kcal/mol are highlighted in bold. B3LYP = B3LYP/6-31+G(d,p)//B3LYP/6-31+G(d,p), mPW1PW91 = mPW1PW91/6-31+G(d,p)//B3LYP/6-31+G(d,p), MPWB1K = MPWB1K/6-31+G(d,p)//B3LYP/6-31+G(d,p). All energies include zero point corrections from B3LYP/6-31+G(d,p). [b]See ref 26a for description of different conformers.

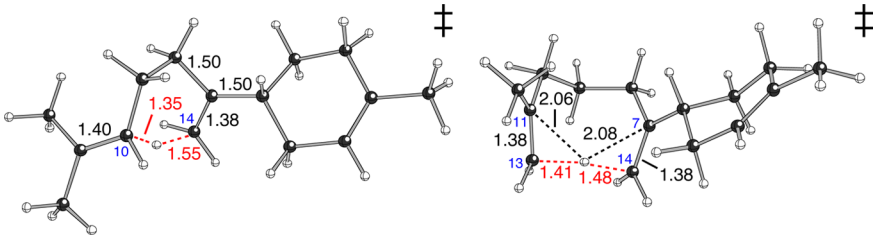

Figure 2. Computed geometries (B3LYP/6-31+G(d,p), distances in Å) for proton-transfer transition-state structures involved in the formation of macrocarpene (left, 1,5-proton transfer) and tenuifolene (right, 1,7-proton transfer).

Scheme 1

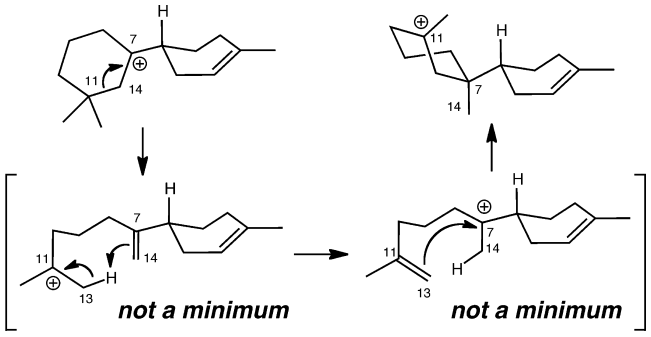

transition-state structure resembles a distorted "proton sandwich,"[13] i.e., the migrating proton interacts with four different carbons (Figure 2, right).

Italicene. Transition-state structures for two proton transfers that could be involved in italicene[14] formation (Figure 1a) are shown in Figure 3. While predicted barriers for both reactions are less than 20 kcal/mol, the 1,6-proton transfer is predicted to be much more facile. These transition-state structures again resemble distorted proton sandwiches, although they are distorted differently (note the geometric relationship between short and long partial bonds).

Aristolochene. A 1,7-proton transfer was also proposed to occur en route to aristolochene (Figure 1a).[15] In 2007,

DOI: 10.1021/ja512685x
J. Am. Chem. Soc. 2015, 137, 4134−4140

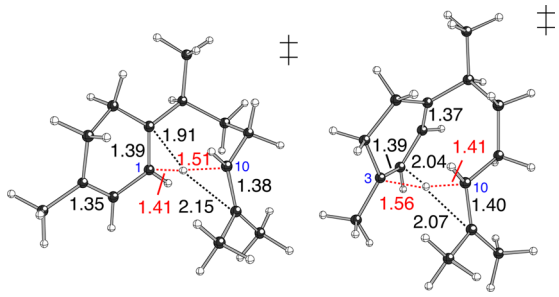

Figure 3. Computed geometries (B3LYP/6-31+G(d,p), distances in Å) for proton-transfer transition-state structures (left, 1,6 and right, 1,8) involved in the formation of italicene.

Allemann, Truhlar, Gao, and co-workers described quantum chemical computations (using DFT, as well as other methods) on this intramolecular proton transfer, predicting a barrier of ~25 kcal/mol in the absence of the enzyme.[16] We predict a similar barrier using different DFT methods (Table 1; as indicated, similar barriers are found for two different conformers; see Figure 4). Results from combined quantum

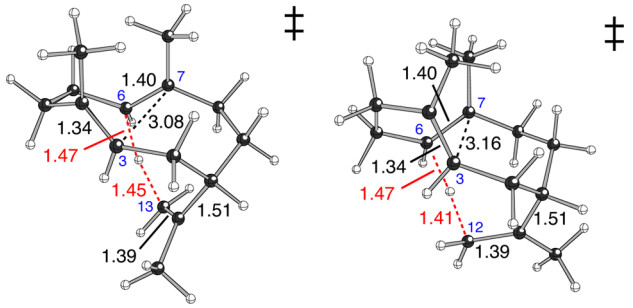

Figure 4. Computed geometries (B3LYP/6-31+G(d,p), distances in Å) for 1,7-proton-transfer transition-state structures (two conformers: left, 1,7-proton transfer (*re/si*) and right, 1,7-proton transfer (*si/si*)) involved in the formation of aristolochene.

mechanics/molecular mechanics (QM/MM) calculations suggested that this barrier could be lowered by 5−7 kcal/mol by the aristolochene synthase enzyme.[16] The resulting barrier is consistent with the barrier expected based on the experimentally measured rate of the aristolochene synthase reaction.[17] Nonetheless, this sort of intramolecular proton transfer is not consistent with previously reported labeling experiments from the Cane group that showed no evidence for the transfer of a proton from carbon 12 to carbon 6.[18] These previous experiments are consistent instead with a mechanism involving deprotonation to form germacrene A and subsequent reprotonation by a different proton (from the enzyme active site). Subsequent labeling experiments by Allemann, Truhlar, Gao, and co-workers confirmed that direct proton transfer from carbon 12 to carbon 6 does not occur in the aristolochene synthase reaction.[19]

Panasinsene. Two 1,5-proton-transfer processes (or 1,6 counting the other way around the large ring) could lead to panasinsene (Figure 1a).[20] Proton transfer from C2 to C6 is predicted to have a barrier of 12−15 kcal/mol (Table 1; Figure 5, left). Proton transfer to the other carbon of the C=C π-bond, C7, is predicted to have much smaller barrier, <5 kcal/mol (Table 1; Figure 5, right). The transition-state structure for proton transfer to C6 (Figure 5, left) is, however, predicted to be connected directly to the carbocation that directly precedes

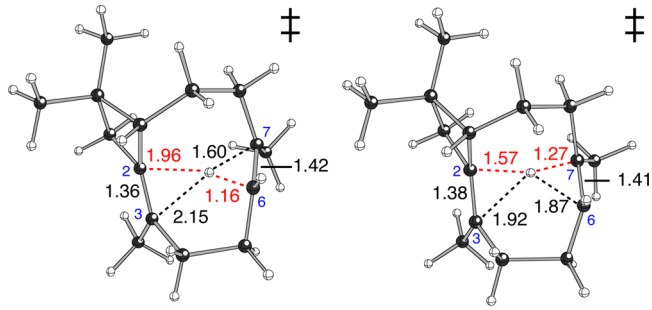

Figure 5. Computed geometries (B3LYP/6-31+G(d,p), distances in Å) for 1,5-proton-transfer transition-state structures involved in the formation of panasinsene (proton transfer to C6 at left, proton transfer to C7 at right).

panasinsene, i.e., proton transfer and subsequent cyclization are combined into a concerted but asynchronous process.[21] Again, these transition-state structures resemble distorted proton sandwiches.

Caryolene. A recent theoretical study on caryolene formation (Figure 1a) described a 1,6-proton-transfer process.[22] This process (proton transfer from C15 to C7) is predicted to have a barrier of >20 kcal/mol (Table 1), which is much larger than the barriers predicted for 1,6-proton transfers involved in italicene and miltiradiene (*vide infra*) formation. However, an alternative deprotonation/reprotonation pathway was predicted to have a much lower barrier.

Taxadiene. DFT calculations on proton-transfer processes potentially involved in taxadiene biosynthesis were described in two papers (Figure 1b).[23] A mechanism involving 1,5-proton transfer (C10 to C6; red in Figure 1b) had been proposed prior to this work[24] and was supported both by labeling experiments that showed that the indicated hydrogen does migrate somehow from carbon 10 to carbon 6 and semiempirical calculations on the reactant and product for this proton-transfer step that indicated that a direct proton transfer was geometrically feasible.[24b] The results of DFT calculations indicate that the direct intramolecular proton transfer is associated with a barrier of only 11−13 kcal/mol (Table 1). An alternative two-step pathway (blue and black in Figure 1b) is predicted to have an overall lower barrier. Thus, it seems possible that the taxadiene-forming reaction may actually involve two sequential 1,5-proton transfers.

Fusicoccadiene. In 2009, Kato and co-workers proposed a mechanism for formation of fusicoccadiene that, like the proposed mechanism for taxadiene formation described above, involves two sequential intramolecular proton transfers.[25] Semiempirical calculations and labeling experiments supporting this proposal were described.[25] The results of our DFT calculations also support the feasibility of the two-step process and indicate that a direct intramolecular proton transfer is also energetically feasible, although less so (Table 1, red in Figure 1b). Computed geometries for the three proton-transfer transition-state structures are shown in Figure 6; the rightmost of these can be formulated as another distorted proton sandwich.

Abietadiene and Miltiradiene. Several theoretical studies on 1,4-proton-transfer processes potentially involved in abietadiene formation (Figure 1c) appeared recently.[26] Calculations with several theoretical methods predict that the barrier for 1,4-proton transfer to either face of the C=C π-bond accepting the proton for either of two conformers of the

DOI: 10.1021/ja512685x
J. Am. Chem. Soc. 2015, 137, 4134−4140

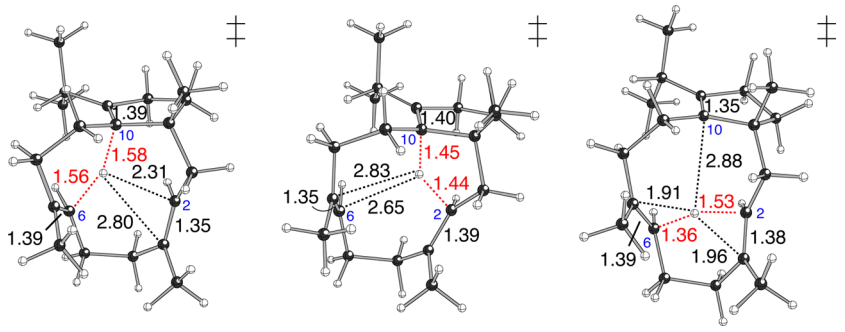

Figure 6. Computed geometries (B3LYP/6-31+G(d,p), distances in Å) for proton-transfer transition-state structures involved in the formation of fusicoccadiene.

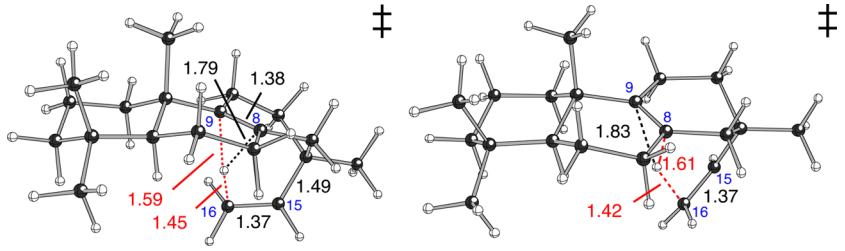

Figure 7. Computed geometries (B3LYP/6-31+G(d,p), distances in Å) for proton-transfer transition-state structures involved in the formation of miltiradiene (1,6-proton transfer at left, 1,5-proton transfer at right).

polycyclic framework ranges from 25 to 33 kcal/mol (see Table 1 for a subset of this data). Direct proton transfer is consistent with labeling experiments,[27] but so would be a deprotonation/reprotonation pathway (involving internal return of the removed proton) that avoids this relatively high barrier. For some conformations, a bifurcation in the reaction coordinate was predicted to occur after the transition-state structure, and direct dynamics calculations were carried out to examine the fate of molecules passing through the region of the proton-transfer transition state.[26b,c] An alternative 1,6-proton transfer productive for miltiradiene formation can also occur (red in Figure 1c; Figure 7, left).[28] This process is predicted to have a barrier less than half that for 1,4-proton transfer (Table 1). In addition, a 1,5-proton transfer with a similar barrier can also occur after an initial 1,2-hydride shift (blue in Figure 1c; Figure 7, right). The potential energy surface connected to these proton-transfer processes is also quite complex (e.g., note that whether or not there is a barrier between the C8−H and C9−H reactants depends on the level of theory; Table 1).[29] The migrating protons in these transition-state structures each interact with three carbons.

Germanicol. An intramolecular proton transfer was also proposed to occur during a biomimetic carbocation cascade utilized by Surendra and Corey to synthesize germanicol and other triterpenes (Figure 1d), who validated their proposal by carrying out a labeling study, the results of which were completely consistent with a direct proton-transfer mechanism.[30] Our DFT calculations also support this proposal, predicting barriers under 10 kcal/mol for 1,5-proton transfer to either face of the C=C π-bond (Table 1 and Figure 8; consistent with the mixture of epimers formed experimentally), again via proton sandwich-like transition-state structures. The alternative 1,4-proton transfer (not observed experimentally) is predicted to have a much larger barrier (Table 1).

General Principles. Can general principles be gleaned from the array of cationic carbon-to-carbon proton-transfer reactions

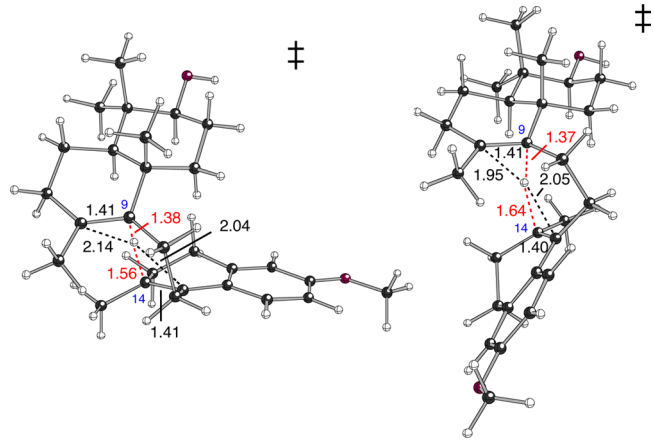

Figure 8. Computed geometries (B3LYP/6-31+G(d,p), distances in Å) for 1,5-proton-transfer transition-state structures involved in the formation of germanicol.

described herein (Figure 9)? Let us consider the influence of several factors on proton-transfer barriers: (1) Ring strain: Simple ring strain arguments would predict that 1,5-proton transfers (i.e., six-membered rings) would be most favorable; overall, they are, with all predicted barriers being lower than 14 kcal/mol. 1,4- and 1,6-proton transfers would be expected to suffer from some strain, but not very much; some of these reactions have low barriers, but others do not (see, for example, factor no. 2). 1,7- and 1,8-proton transfers would be expected to suffer from somewhat larger strain, and these reactions are indeed predicted to have comparatively high barriers. Overall, there appears to be a loose correlation between barrier height and ring size.[31] (2) Degree of substitution: In that both carbocations and alkenes are expected to be "more stable" when more substituted, a correlation between barriers and the degrees of substitution at the carbons between which the proton migrates might be expected. While such a relationship

DOI: 10.1021/ja512685x
J. Am. Chem. Soc. 2015, 137, 4134−4140

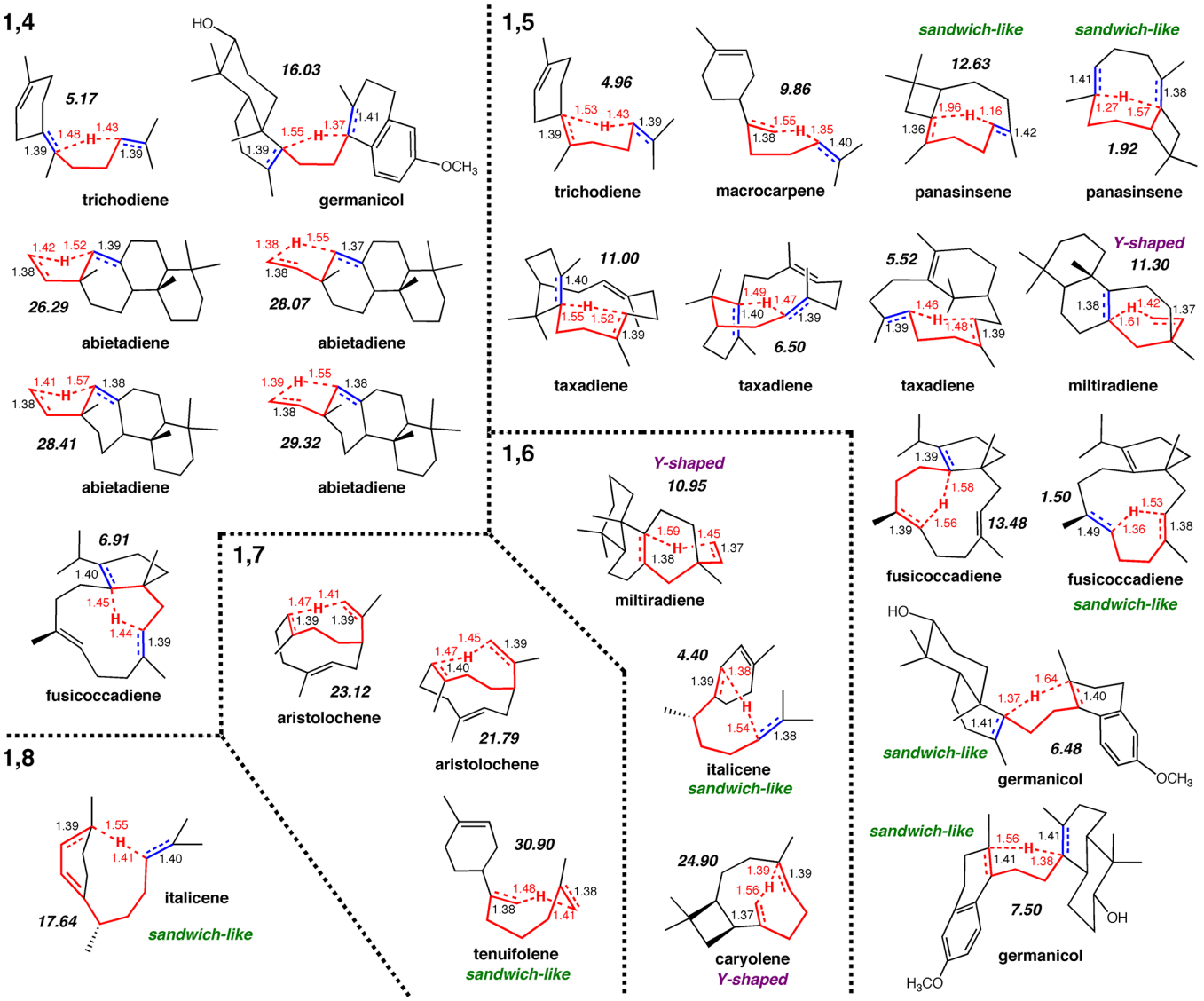

Figure 9. Summary of transition-state structure geometries (B3LYP/6-31+G(d,p)) for all intramolecular proton transfers discussed. Distances are shown in Å. Predicted barriers (mPW1PW91/6-31+G(d,p)//B3LYP/6-31+G(d,p)) are shown next to each structure. The cycle transiently formed during proton transfer is highlighted in red for each structure. Partial double bonds within this cycle are shown in red, while those exocyclic with respect to this cycle are shown in blue. Structures with sandwich-like C/C/H/C/C arrays are labeled in green. Structures with Y-shaped C/C/H arrays are labeled in purple.

does not appear to dominate the reactivity predicted by our calculations, most of the highest predicted barriers within the 1,4- and 1,5-proton-transfer groups involve a monosubstituted carbon. (3) Endo vs exo: In general, it appears that having more exocyclic partial double bonds in a proton-transfer transition-state structure leads to a lower barrier.[31,32] (4) Sandwich delocalization: The delocalization in the transition-state structures is of three types: linear C···H···C, "Y-shaped" where the proton interacts (with distances ~2.2 Å or less) with three carbons, and "sandwich-like" where the proton interacts (with distances ~2.2 Å or less) with four carbons. While some of the lowest predicted proton-transfer barriers involve sandwich-like delocalization, so do some of the highest, suggesting that the presence or absence of this type of delocalization is not predictive on its own. (5) Other factors: For some systems, additional factors play key roles. For example, the predicted barrier for panasinene is likely one of the highest 1,5-proton-transfer barriers due to the strain associated with converting an sp^3 carbon of its four-membered ring into an sp^2 carbon. A different effect contributes to the relatively low barrier (compared, for example, to all of the 1,7-proton-transfer barriers) for the 1,8-proton transfer en route to italicene—the formation of an allylic cation.

CONCLUSIONS

In summary, we recommend that direct, i.e., intramolecular, proton-transfer mechanisms be considered for terpene-forming carbocation rearrangements involving net 1,4-, 1,5-, or 1,6-proton transfers, especially when exocyclic π-systems (as defined above) are involved and migration to or from a methylene group is not. Beyond these simple considerations, firm predictions require quantum chemical calculations, since proton-transfer barriers are modulated by a variety of factors. The results described herein do not rule out deprotonation/reprotonation mechanisms, which could exist as preferred alternatives or could occur along with direct proton transfers in

DOI: 10.1021/ja512685x
J. Am. Chem. Soc. 2015, 137, 4134−4140

different turnover steps for a given enzyme. Our results do, however, lead to clear predictions as to cases where intramolecular proton transfers have low enough barriers to occur without enzymatic intervention and cases where intervention is a necessity.

■ ASSOCIATED CONTENT

Supporting Information

Coordinates and energies for all computed structures, data for small model systems, full Gaussian citations. This material is available free of charge via the Internet at http://pubs.acs.org.

■ AUTHOR INFORMATION

Corresponding Author

*djtantillo@ucdavis.edu

Notes

The authors declare no competing financial interest.

■ ACKNOWLEDGMENTS

We gratefully acknowledge support from UC Davis and the National Science Foundation (CHE-0449845, CHE-0957416, and CHE030089 for supercomputing resources).

■ REFERENCES

(1) For leading references, see: (a) Christianson, D. W. *Curr. Opin. Chem. Biol.* **2008**, *12*, 141−150. (b) Christianson, D. W. *Chem. Rev.* **2006**, *106*, 3412−3442. (c) Davis, E. M.; Croteau, R. *Top. Curr. Chem.* **2000**, *209*, 53−95. (d) Cane, D. E. *Compr. Nat. Prod. Chem* **1999**, *2*, 155−200. (e) Cane, D. E. *Chem. Rev.* **1990**, *90*, 1089−1103.

(2) Frisch, M. J. et al. *Gaussian 03*, revision D.01; Gaussian, Inc.: Pittsburgh, PA, 2003. Frisch, M. J. et al. *Gaussian 09*, revision B.01; Gaussian, Inc.: Pittsburgh, PA, 2010 (full references in Supporting Information).

(3) (a) Becke, A. D. *J. Chem. Phys.* **1993**, *98*, 5648−5652. (b) Becke, A. D. *J. Chem. Phys.* **1993**, *98*, 1372−1377. (c) Lee, C.; Yang, W.; Parr, R. G. *Phys. Rev. B* **1988**, *37*, 785−789. (d) Stephens, P. J.; Devlin, F. J.. (e) Chabalowski, C. F.; Frisch, M. J. *J. Phys. Chem.* **1994**, *98*, 11623−11627.

(4) (a) Gonzalez, C.; Schlegel, H. B. *J. Phys. Chem.* **1990**, *94*, 5523−5527. (b) Fukui, K. *Acc. Chem. Res.* **1981**, *14*, 363−368.

(5) Matsuda, S. P. T.; Wilson, W. K.; Xiong, Q. *Org. Biomol. Chem.* **2006**, *4*, 530−543.

(6) (a) Zhao, Y.; Truhlar, D. G. *J. Phys. Chem. A* **2004**, *108*, 6908−6918. (b) Zheng, J.; Zhao, Y.; Truhlar, D. G. *J. Chem. Theory Comput.* **2007**, *3*, 569−582.

(7) Tantillo, D. J. *Nat. Prod. Rep.* **2011**, *28*, 1035−1053.

(8) Müller, N.; Falk, A.; Gsaller, G. *Ball & Stick V.4.0a12, molecular graphics application for MacOS computers*; Johannes Kepler University: Linz, Austria, 2004.

(9) Hong, Y. J.; Tantillo, D. J. *Org. Lett.* **2006**, *8*, 4601−4604.

(10) For leading references, see: (a) Vedula, L. S.; Cane, D. E.; Christianson, D. W. *Biochemistry* **2005**, *44*, 12719−12727. (b) Rynkiewicz, M. J.; Cane, D. E.; Christianson, D. W. *Biochemistry* **2002**, *41*, 1732−1741. (c) Rynkiewicz, M. J.; Cane, D. E.; Christianson, D. W. *Proc. Natl. Acad. Sci. U.S.A.* **2001**, *98*, 13543−13548. (d) Cane, D. E. *Pure. Appl. Chem.* **1989**, *61*, 493−496.

(11) (a) Hong, Y. J.; Tantillo, D. J. *Org. Biomol. Chem.* **2009**, *7*, 4101−4109. (b) See also: Hong, Y. J.; Tantillo, D. J. *J. Am. Chem. Soc.* **2014**, *136*, 2450−2463.

(12) (a) Kollner, T. G.; Schnee, C.; Li, S.; Svatos, A.; Schneider, B.; Gershenzon, J.; Degenhardt, J. *J. Biol. Chem.* **2008**, *283*, 20779−10788. (b) Kreipl, A. T.; König, W. A. *Phytochemicals* **2004**, *65*, 2045−2049.

(13) (a) Gutta, P.; Tantillo, D. J. *Angew. Chem., Int. Ed.* **2005**, *44*, 2719−2723. (b) Ponec, R.; Bultinck, P.; Gutta, P.; Tantillo, D. J. *J. Phys. Chem. A* **2006**, *110*, 3785−3789. (c) Tantillo, D. J. *Chem. Soc. Rev.* **2010**, *39*, 2847−2854.

(14) Leimner, J.; Marschall, H.; Meier, N.; Weyerstahl, P. *Chem. Lett.* **1984**, 1769−1772.

(15) Noguchi, H.; Rawlings, B. J. *J. Am. Chem. Soc.* **1989**, *111*, 8914−8916.

(16) Allemann, R. K.; Young, N. J.; Ma, S.; Truhlar, D. G.; Gao, J. *J. Am. Chem. Soc.* **2007**, *129*, 13008−13013.

(17) Deligeorgopoulou, A.; Taylor, S. E.; Forcat, S.; Allemann, R. K. *Chem. Commun.* **2003**, 2162−2163.

(18) Cane, D. E.; Prabhakaran, P. C.; Oliver, J. S.; McIlwaine, D. B. *J. Am. Chem. Soc.* **1990**, *112*, 3209−3210.

(19) Miller, D. J.; Gao, J.; Truhlar, D. G.; Young, N. J.; Gonzalez, V.; Allemann, R. K. *Org. Biomol. Chem.* **2008**, *6*, 2346−2354.

(20) Yoshihara, K.; Hirose, Y. *Bull. Chem. Soc. Jpn.* **1975**, *48*, 2078−2080.

(21) (a) Tantillo, D. J. *J. Phys. Org. Chem.* **2008**, *21*, 561−570. (b) Williams, A. *Concerted Organic and Bio-Organic Mechanisms*; CRC Press: Boca Raton, 2000. (c) Hess, J. B. A. *J. Am. Chem. Soc.* **2002**, *124*, 10286−10287.

(22) Nguyen, Q. N. N.; Tantillo, D. J. *Beilstein J. Org. Chem.* **2013**, *9*, 323−331.

(23) (a) Gutta, P.; Tantillo, D. J. *Org. Lett.* **2007**, *9*, 1069−1071. (b) Hong, Y. J.; Tantillo, D. J. *J. Am. Chem. Soc.* **2011**, *133*, 18249−18256.

(24) For leading references, see: (a) Lin, X.; Hezari, M.; Koepp, A. E.; Floss, H. G.; Croteau, R. *Biochemistry* **1996**, *35*, 2968−2977. (b) Williams, C. D.; Carroll, B. J.; Jin, Q.; Rithner, C. D.; Lenger, S. R.; Floss, G. H.; Coates, R. M.; Williams, R. M.; Croteau, R. *Chem. Biol.* **2000**, *7*, 969−977. (c) Chow, S. Y.; Williams, H. J.; Huang, Q.; Nanda, S.; Scott, A. I. *J. Org. Chem.* **2005**, *70*, 9997−10003.

(25) Toyomasu, T.; Tsukahara, M.; Kenmoku, H.; Anada, M.; Nitta, H.; Ohkanda, J.; Mitsuhashi, W.; Sassa, T.; Kato, N. *Org. Lett.* **2009**, *11*, 3044−3047.

(26) (a) Hong, Y. J.; Tantillo, D. J. *Nat. Chem.* **2009**, *1*, 384−389. (b) Siebert, M. R.; Zhang, J.; Addepalli, S. V.; Tantillo, D. J.; Hase, W. L. *J. Am. Chem. Soc.* **2011**, *133*, 8335−8343. (c) Siebert, M. R.; Paranjothy, M.; Sun, R.; Tantillo, D. J.; Hase, W. L. *J. Chem. Theory Comput.* **2012**, *8*, 1212−1222.

(27) For leading references, see: Ravn, M. M.; Peters, R. J.; Coates, R. M.; Croteau, R. *J. Am. Chem. Soc.* **2002**, *124*, 6998−7006.

(28) For leading references, see: Zhou, Y. J.; Gao, W.; Rong, Q.; Jin, G.; Chu, H.; Liu, W.; Yang, W.; Zhu, Z.; Li, G.; Zhu, G.; Huang, L.; Zhao, Z. K. *J. Am. Chem. Soc.* **2012**, *134*, 3234−3241.

(29) Hong, Y. J.; Tantillo, D. J. *Nat. Chem.* **2014**, *6*, 104−111.

(30) Surendra, K.; Corey, E. J. *J. Am. Chem. Soc.* **2008**, *130*, 8865−8869. During their synthetic studies, these authors observed what they described as, "a highly unusual acyclic, 1,5-migration of a proton... This is a rare (and possibly unprecedented) example of such an intramolecular rearrangement". As shown herein, however, there was actually ample precedent for the feasibility of such processes in terpene biosynthesis.

(31) This conclusion is supported by calculations on small model systems. See Supporting Information for details.

(32) Note that transition-state structures examined herein generally involve geometries that are allowed by or fall outside of those covered by Baldwin's rules. A recent review: Alabugin, I. V.; Gilmore, K. *Chem. Commun.* **2013**, *49*, 11246−11250.

DOI: 10.1021/ja512685x
J. Am. Chem. Soc. 2015, 137, 4134−4140